Quantum kinetic study of the electron-LO-phonon interaction in a semiconductor

J. A. Kenrow
Department of Physics, University of Florida, Gainesville, Florida 32611
(Received 9 May 1996; revised manuscript received 1 October 1996)

We present a full quantum-mechanical study of the early time kinetics of a coupled electron-LO-phonon system in a semiconductor quantum wire. Schrödinger's equation is directly solved to obtain the many-body wave function for a conduction electron interacting with the complete spectrum of phonon modes. This approach has the advantage of treating the electron and the phonons as well as their correlation on equal footing and as interdependent entities. We show that the electron and phonon observables illustrate the non-Markovian nature of the early time kinetics, namely, a retarded loss of the electron's momentum and an initial overshoot in it's kinetic energy. These effects are shown to stem from the buildup of correlation between the electron and the phonons and are mediated by virtual transitions. It is shown further that the continuous nature of the electron-phonon interaction has important consequences in both the electron's relaxation and transport behavior, e.g., the suppression of scattering in strong longitudinal electric fields. The quantum kinetic results are compared to those obtained from a traditional semiclassical treatment. [S0163-1829(97)00712-1]

I. INTRODUCTION

The electron-LO-phonon interaction is one of the most fundamental interactions in semiconductor carrier kinetics. It is the central mechanism that governs carrier relaxation in semiconductor transport. For the semiclassical regime, i.e., the long time limit, the role of LO-phonon emission in semiconductor carrier kinetics is well understood.[1] Kinetic theories for the long time limit are based on the semiclassical Boltzmann equation which contains scattering integrals to describe the interaction between the electrons and the lattice.[2–5] In semiclassical kinetics the Boltzmann scattering integrals are derived under the assumptions that (i) an electron-phonon scattering event is instantaneous or at least is completed on a time scale much faster than the temporal spacing between successive collisions, and (ii) the electron is essentially a free particle between collisions. It follows that collisions are independent events and individually conserve energy. The temporal spacing between successive collisions is set by the probability for an electron to scatter ''into'' and ''out of'' a momentum state k. These in- and out-scattering rates are determined from Fermi's golden rule. For LO-phonon emission in GaAs the inverse scattering rate is $\tau_{\mathrm{LO}} \sim$ 100 fs.[1,6] For times $t > \tau_{\mathrm{LO}}$, this coarse-grain description for the collisions works well and the semiclassical Boltzmann equation in this case is regarded as an essential tool for predicting carrier kinetics in semiconductors.[3,5,7]

The growing trend towards nanometer length scales in semiconductor devices leads to very large electric fields in the active region. This in turn leads to a quantum transport regime in which the characteristic times imposed by the high fields approach time scales defined by the time-energy uncertainty. It is well known that large electric field strengths in semiconductors can cause appreciable changes in the carrier distribution for times $t \lesssim \tau_{\mathrm{LO}}$. Similarly, in semiconductor optics, ultrashort laser pulses can create carriers over a time interval as small as 6 fs.[8–10] In both of these cases the carrier kinetics are governed, to a large extent, by quantum mechanics rendering the semiclassical energy conserving pair-scattering description invalid because a coarse-grain collision description fails to capture the underlying physics of the interaction. For early times ($t \lesssim \tau_{\mathrm{LO}}$), one cannot ignore that the electron-phonon interaction is a *continuous* process and that the electron is not in a well-defined state. Further, in high electric fields, the electron will accelerate appreciably during the interaction process, requiring that the electron-phonon scattering and the acceleration in the electric field cannot be treated as separate entities.

Extensions of the semiclassical Boltzmann equation have been proposed and applied to semiconductor systems which incorporate the so-called collision duration, collisional broadening, and intracollisional field effect on an approximate level to account for the quantum effects mentioned above.[11–14] However, proper inclusion of these effects in a semiclassical kinetic theory is nontrivial. As an example, the improper inclusion of collisional broadening leads to a violation of the conservation laws.

The short time-scale effects of the electron-phonon interaction are naturally accounted for in a quantum kinetic theory. In recent years, quantum kinetic equations have been derived using reduced density matrices[15–17] and the Keldysh nonequilibrium Green's functions.[18–21] However, to obtain a closed set of kinetic equations for the one-particle expectation values, additional approximations are required. In the case of the reduced density matrices, one has to break the hierarchy of equations of motion and retain only the coupling to the next order correlation in some phenomenological (Markovian) manner.[17] In the case of nonequilibrium Green's functions, one has to choose an approximation for the self-energy and further use the generalized Kadanoff-Baym anzatz to reduce the two-timed, kinetic nonequilibrium Green's function to the one-timed density matrices.[19,22] The simplifying approximations in both of these approaches leads to some loss in correlation, the implications of which are not well understood.

The many-particle Schrödinger equation, although limited to simple model systems in condensed matter, provides an alternative and perhaps most intuitive approach to quantum

kinetics since *all* the quantum mechanics of the system, in particular, the correlations, are contained in the many-body wave function. Recently we introduced a wave function approach for the quantum kinetics of a model coupled electron-LO-phonon system in a semiconductor.[23] Contrary to the common belief in condensed matter many-body theory, we showed that direct computation of the many-body wave function is feasible in the early time kinetic regime. In this paper we apply this method to investigate the microscopic details of the electron-LO-phonon interaction and the consequences it has on the kinetics of a single conduction band electron with and without the presence of an external longitudinal electric field. We expand the theory in Ref. 23 to include a longitudinal electric field. Our investigation of the interacting system is illustrated through the dynamics of the electron, the phonons, and the electron-phonon correlation. Unlike many kinetic studies in semiconductors, the phonons here are treated as a dynamic entity. To our knowledge this is the first investigation of kinetics in which the electron, phonons, and their correlation are treated on an equal footing *and* as interdependent entities. As a basis for comparison, the quantum kinetic results are compared to those obtained from the semiclassical Boltzmann equation.

The paper is organized as follows: In Sec. II the coupled electron-LO-phonon system is described and the formalization of the full many-body wave function is presented. A brief presentation of the semiclassical Boltzmann equation used in the comparison with the quantum kinetic model is given in Sec. III. In Sec. IV numerical results of the electron and phonon observables from the quantum kinetic theory are presented and compared to the corresponding semiclassical results. Discussions are included. Concluding remarks are made in Sec. V. An example calculation demonstrating the time evolution of the phonon distribution is presented in Appendix A. Lastly, an analytical calculation of the electron-LO-phonon correlation energy for the very early times is presented in Appendix B.

II. QUANTUM KINETIC MODEL

Our model system consists of a single quasi-one-dimensional conduction band electron coupled to the complete spectrum of one dimensional (1D) LO-phonon modes in a semiconductor quantum wire. The wire cross section $(l_x \times l_y)$ lies in the x,y plane and the wire length along the z coordinate. We restrict our study to intrasubband transitions and thus assume that the electron remains in the lowest transversal subband eigenstate of the wire. We are then left with an effective 1D problem where the coupled electron-LO-phonon system is represented by the longitudinal wave function, $|\psi(z,t)\rangle$, where the *ket* denotes the phonon at time t given that the electron is at position z.

The many-body wave function, $|\psi(z,t)\rangle$, is time evolved within the effective mass approximation according to Schrödinger's equation,

$$i\hbar \frac{\partial |\psi\rangle}{\partial t} = \hat{H}_{\rm tot}|\psi\rangle = (\hat{H}_e + \hat{H}_{\rm ph} + \hat{H}_{e-{\rm ph}})|\psi\rangle, \qquad (2.1)$$

where $\hat{H}_e$ and $\hat{H}_{\rm ph}$ are the respective noninteracting electron and phonon Hamiltonian operators and $\hat{H}_{e-{\rm ph}}$ is the effective 1D Fröhlich electron-phonon interaction Hamiltonian operator for a rectangular quantum wire,[6,24,25] all given, respectively, by

$$\hat{H}_e(z) = -\frac{\hbar^2}{2m}\frac{\partial^2}{\partial z^2} + V_F(z), \qquad (2.2)$$

$$\hat{H}_{\rm ph} = \hbar\omega \sum_l^N (a_{q_l}^\dagger a_{q_l} + 1/2), \qquad (2.3)$$

and

$$\hat{H}_{e-{\rm ph}}(z) = S\sum_l \frac{1}{Q_l}[a_{q_l} e^{iq_l z} - a_{q_l}^\dagger e^{-iq_l z}], \qquad (2.4)$$

where

$$Q_l = \left[q_l^2 + \left(\frac{\pi}{l_x}\right)^2 + \left(\frac{\pi}{l_y}\right)^2 \right]^{1/2}, \qquad (2.5)$$

and S is the effective 1D coupling constant defined by

$$S = 2i\left[\frac{e^2\hbar\omega}{2\epsilon_0\Omega}\left(\frac{1}{\epsilon_\infty} - \frac{1}{\epsilon_s}\right)\right]^{1/2}, \qquad (2.6)$$

(note that S is defined imaginary). In Eqs. (2.2)–(2.6), N denotes the number of phonon modes, m is the electron effective mass, the longitudinal potential is given by $V_F = -ezF$, where F is the corresponding dc electric field, Ω is the normalization volume, ϵ_s and ϵ_∞ are, respectively, the static and optical relative dielectric constants, and $a_{q_l}^\dagger$ (a_{q_l}) denote the creation (annihilation) operators for the LO phonons. The phonons are assumed to be dispersionless with a fixed energy of $\hbar\omega$. We define q_l as the z-component phonon wave number of the lth phonon mode corresponding to the z coordinate along the wire (k is the corresponding z-component wave number of the electron). We assume an uncorrelated initial state for the electron-phonon system which implies weak coupling. At $t=0$, the electron description is given by a Gaussian wave packet along z with a specified wave number k_i. The lattice at $t=0$ is taken as the vacuum state for the LO phonons.

We point out that Eq. (2.1) is not the *single-electron* Schrödinger equation, but rather represents the time evolution of the *many-body* state vector, $|\psi(z,t)\rangle$, of one electron and many phonons. In an interacting system, $|\psi(z,t)\rangle$ is not separable in the electron and phonon coordinates and it contains *all* the correlations (phase relations) between the electron and phonons.

The many-body wave function in Eq. (2.1) can be written as a linear superposition over the orthonormal basis of LO-phonon number states,[23]

$$|\psi(z,t)\rangle = \alpha(z,t)|0\rangle + \sum_l^N \beta_l(z,t)e^{-i\omega t}|1\rangle_l + \sum_{l,\ m\geq l}^N \gamma_{lm}(z,t)e^{-i2\omega t}|2\rangle_{lm} + \cdots, \qquad (2.7)$$

where $|0\rangle$ represents the lattice vacuum state, $|1\rangle_l$ and $|2\rangle_{lm}$ represent, respectively, the first- and second-order number states. All the electronic information is contained in

the coefficients α, β_l, and γ_{lm}. The ordering of the phonon mode occupancies in the various number states is illustrated through the number state symbols, i.e., $|1\rangle_l$ represents the distinct first-order number state with an occupancy of **1** in the lth LO-phonon mode. All the possible second-order number states, $|2\rangle_{lm}$, span the $l\times m$ matrix which for $l=m$, $|2\rangle_{ll}$ represents the lattice state with an occupancy of **2** in the lth LO-phonon mode and for $l\neq m$, $|2\rangle_{lm}$ represents the lattice state with an occupancy of **1** in both the lth and mth LO-phonon modes. To avoid duplicate counting and to ensure distinct second-order states, it is required that $m\geqslant l$. It follows that for a system of N phonon modes, there are N distinct combinations of first-order number states, $|1\rangle_l$, and $N(N+1)/2$ distinct combinations of second-order number states, $|2\rangle_{lm}$.

The final set of coupled kinetic equations for $\alpha(z,t)$, $\beta_l(z,t)$, and $\gamma_{lm}(z,t)$ are obtained by applying the Hamiltonian operators defined by Eqs. (2.2)–(2.4) on $|\psi(z,t)\rangle$, and then projecting them onto each unique number state:

$$\frac{\partial\alpha}{\partial t}=\frac{1}{i\hbar}\left[-\frac{\hbar^2}{2m}\frac{\partial^2}{\partial z^2}+V_F\right]\alpha+\frac{Se^{-i\omega t}}{i\hbar}\sum_l\frac{e^{iq_lz}}{Q_l}\beta_l, \quad (2.8)$$

$$\frac{\partial\beta_l}{\partial t}=\frac{1}{i\hbar}\left[-\frac{\hbar^2}{2m}\frac{\partial^2}{\partial z^2}+V_F\right]\beta_l-\frac{Se^{i(\omega t-q_lz)}}{i\hbar Q_l}\alpha+\frac{Se^{-i\omega t}}{i\hbar}\times\left[\frac{e^{iq_lz}}{Q_l}\sqrt{2}\,\gamma_{ll}+\left(\sum_{\substack{m\\ m<l}}^{N}\gamma_{ml}+\sum_{\substack{m\\ m>l}}^{N}\gamma_{lm}\right)\frac{e^{iq_mz}}{Q_m}\right], \quad (2.9)$$

$$\frac{\partial\gamma_{lm}}{\partial t}=\frac{1}{i\hbar}\left[-\frac{\hbar^2}{2m}\frac{\partial^2}{\partial z^2}+V_F\right]\gamma_{lm}-\frac{\sqrt{2}Se^{i(\omega t-q_lz)}}{i\hbar Q_l}\beta_l\delta_{lm}-\frac{Se^{i\omega t}}{i\hbar}\left[\frac{e^{-iq_lz}}{Q_l}\beta_m+\frac{e^{-iq_mz}}{Q_m}\beta_l\right]\overline{\delta_{lm}}+\cdots, \quad (2.10)$$

where δ_{lm} is the Kronecker δ function and we define $\overline{\delta_{lm}}\equiv 1$, for $l\neq m$, as the ''anti-'' Kronecker δ function. In obtaining Eqs. (2.8)–(2.10), the following Boson creation and annihilation operator relations were used:

$$a_{q_l}|0\rangle=0,$$

$$a^{\dagger}_{q_l}|0\rangle=|1\rangle_l,$$

$$a_{q_l}|1\rangle_{l'}=\delta_{ll'}|0\rangle,$$

$$a^{\dagger}_{q_l}|1\rangle_{l'}=\begin{cases}|2\rangle_{ll'} & \text{for } l'>l\\ \sqrt{2}\,|2\rangle_{ll} & \text{for } l=l'\\ |2\rangle_{l'l} & \text{for } l'<l,\end{cases}$$

$$a_{q_l}|2\rangle_{l'm'}=\delta_{l'm'}[\sqrt{2}\,\delta_{ll'}|1\rangle_{l'}]+\overline{\delta_{l'm'}}[\delta_{ll'}|1\rangle_{m'}+\delta_{lm'}|1\rangle_{l'}].$$

Equations (2.8)–(2.10) have complete time reversal symmetry. In contrast to Boltzmann kinetics, where all phase coherence is destroyed after one single scattering event, the phase coherence here is *never* lost but instead distributed over a large number of phonon modes.

It was shown in Ref. 23 that coupling to the next higher order number state in Eqs. (2.8)–(2.10) is retarded by a time $t\sim(S/\hbar Q_l)^{-1}|_{q_l=0}$. In the case considered here, this retardation time is 400 fs. It then follows that for small coupling strengths and small times the trajectory of the full many-body system is confined to the subspace of **0**, **1**, and **2** phonon number states. Making use of this fact, the full Hamiltonian in Eq. (2.1) can be replaced by its projection onto the subspace of **0, 1**, and **2** phonon number states, $\hat{H}_{\rm tot}\rightarrow P\hat{H}_{\rm tot}P$, where P is the projection operator defined by

$$P|0\rangle=|0\rangle;\quad P|1\rangle_l=|1\rangle_l;\quad P|2\rangle_{lm}=|2\rangle_{lm}$$

and

$$P|n\rangle=0\quad\text{for } n\geqslant 3.$$

In this subspace the problem is exactly solvable. We note that this projection onto a finite number of degrees of freedom leads to a closed system where the kinetics can never truly be dissipative. On very short times, however, the kinetics of this closed system are indistinguishable from true dissipative kinetics with infinite degrees of freedom.

The spontaneous emission and absorption of LO phonons and the external electric field are all strongly coupled processes in Eqs. (2.8)–(2.10). In the wave function approach it is impossible to decouple the two types of scattering processes as well as the effects from an external electric field because the effects of an interaction Hamiltonian on the wave function are described as a single entity and cannot be dissected into parts, as it is done in semiclassical kinetics. This dissection of the interaction is the reason for the intrinsic difficulty of proper descriptions of the intracollisional field effect, collisional broadening, and collision duration in semiclassical kinetic theories.

Equations (2.8)–(2.10) are solved to obtain the wave function $|\psi(z,t)\rangle$ of the coupled electron-phonon system and hence the density operator $\hat{\rho}(z,t)=|\psi(z,t)\rangle\langle\psi(z,t)|$. The electronic probability density is then formed by taking a partial trace over the lattice coordinates,

$$\rho_e(z,t)=\mathrm{Tr}_L[\hat{\rho}(z,t)]=|\alpha(z,t)|^2+\sum_l^N|\beta_l(z,t)|^2+\sum_{l,\ m\geqslant l}^{N}|\gamma_{lm}(z,t)|^2. \quad (2.11)$$

Similarly, $\rho_e(k,t)$ is obtained from $\hat{\rho}(z,t)$ by taking the Fourier transform, $|\psi(k,t)\rangle=\mathcal{F}[|\psi(z,t)\rangle]$. From $\rho_e(k,t)$ the average electron wave number $\langle k\rangle$, and average electron kinetic energy $\epsilon_{\rm el}=\langle\epsilon_k\rangle=\langle\hbar^2k^2/2m\rangle$, are readily calculated as functions of time. We demonstrate the calculation for the time evolved phonon probability distribution, $\rho_{\rm ph}(k,t)$, in a simple example given in Appendix A.

The presented quantum kinetic theory ensures energy conservation of the coupled electron-phonon system. In the absence of an external electric field, the total energy of the system is given by the initial electron energy, E_i, such that

$$E_{\rm tot}=E_i=\epsilon_{\rm el}+\epsilon_{\rm ph}+\epsilon_c\,, \tag{2.12}$$

with

$$\epsilon_{\rm el}=\langle\psi|\hat{H}_e|\psi\rangle=\sum_k\ \epsilon_k\rho_e(k,t), \tag{2.13}$$

$$\epsilon_{\rm ph}=\langle\psi|\hat{H}_{\rm ph}|\psi\rangle=\sum_k\ \left[\hbar\omega\sum_l^N\ |\beta_l(k,t)|^2 + 2\hbar\omega\sum_{l,\ m\geq l}^{N}\ |\gamma_{lm}(k,t)|^2\right], \tag{2.14}$$

$$\epsilon_c=\langle\psi|\hat{H}_{e-{\rm ph}}|\psi\rangle, \tag{2.15}$$

where $\epsilon_{\rm el}$, $\epsilon_{\rm ph}$, and ϵ_c are, respectively, the electron kinetic energy, the ''free'' phonon energy and the interaction (correlation) energy between the electron and the LO phonons. An analytical expression for the early time perturbative expansion of ϵ_c is given in Appendix B.

III. SEMICLASSICAL KINETIC MODEL

For a basis of comparison we solve the semiclassical Boltzmann equation for the model single-band electron-LO-phonon system presented in Sec. II. For the sake of simplicity we neglect here the dynamics of the phonon system. In the presence of an external dc electric field along the wire and for $T=0$ K the Boltzmann equation for the electron is given as

$$\left[\frac{\partial}{\partial t}-\frac{eF}{\hbar}\nabla_k\right]f_k=\frac{2\pi}{\hbar}\sum_{k'}\ g^2(|k-k'|) \times[\,\delta(\epsilon_k-\epsilon_{k'}+\hbar\omega)(1-f_k)f_{k'} - \delta(\epsilon_k-\epsilon_{k'}-\hbar\omega)f_k(1-f_{k'})], \tag{3.1}$$

where f_k is the electron distribution function, F is the external dc electric field, and g is the electron-LO-phonon coupling for the rectangular quantum wire given by[6]

$$g^2(|k-k'|)=\frac{8\left(\frac{8}{3\pi}\right)^4e^2\hbar\omega}{Ll_xl_y\epsilon_0}\left(\frac{1}{\epsilon_\infty}-\frac{1}{\epsilon_s}\right) \times\left[\frac{1}{(|k-k'|)^2+\left(\frac{\pi}{l_x}\right)^2+\left(\frac{\pi}{l_y}\right)^2}\right]. \tag{3.2}$$

We rewrite Eq. (3.1) by letting $\Sigma_{k'}\rightarrow L/2\pi\int_{-\infty}^{\infty}dk'$ and evaluating the energy conserving δ functions,

$$\left[\frac{\partial}{\partial t}-\frac{eF}{\hbar}\nabla_k\right]f_k=\sqrt{\frac{m}{2}}\frac{L}{\hbar^2}\{[g^2(|k-\kappa^+|)(1-f_k)f_{\kappa^+} + g^2(|k+\kappa^+|)(1 - f_k)f_{-\kappa^+}]D(\epsilon_{\kappa^+})\Theta(\kappa^+) - [g^2(|k-\kappa^-|)f_k(1-f_{\kappa^-}) + g^2(|k+\kappa^-|) \times f_k(1-f_{-\kappa^-})]D(\epsilon_{\kappa^-})\Theta(\kappa^-)\}, \tag{3.3}$$

where L is the normalizing wire length, $\kappa^{\pm}=\sqrt{k^2\pm 2m\omega/\hbar}$ and $\epsilon_{\kappa^{\pm}}=(\hbar\kappa^{\pm})^2/2m$ are the respective momenta and energies of the phonon replicas of a given k state, and $D(\epsilon)=(\epsilon)^{-1/2}$ is the 1D density of states. We incorporate a broadening term, similar to Briggs *et al.*,[26] to overcome the singularity located at the LO-phonon threshold, $\epsilon_{\rm el}=\hbar\omega$, in the 1D density of final states, $D(\epsilon_{\kappa^-})$. Equation (3.3) is solved using a moving frame[27] through the coordinate transformation $\tilde{t}=t$, where $\tilde{k}=k+(e/\hbar)Ft$ is the corresponding quasimomentum which obeys the so-called acceleration theorem, $(\partial/\partial t)\tilde{k}=(e/\hbar)F$.

IV. NUMERICAL RESULTS AND DISCUSSION

In this section, we present numerical results for the electron and phonon observables with and without an external longitudinal dc electric field along the wire. From the quantum kinetic theory (QK), the average electron wave number $\langle k\rangle$, the average electron kinetic energy $\epsilon_{\rm el}$, as well as the electron and phonon probability densities, ρ_e and $\rho_{\rm ph}$, are extracted from the many-body wave function which is computed by numerical integration of Eqs. (2.8)–(2.10). The corresponding results from the semiclassical kinetic theory (SC) are obtained from the electron distribution function, $f_k=f(k,t)$, by numerical integration of Eq. (3.3). For the GaAs wire we used material parameters ($m=0.067m_e$, $\hbar\omega=36.2$ meV, $\epsilon_s=13.1$, $\epsilon_\infty=10.9$, and $l_x=l_y=60$ Å). The constraint of the initial lattice vacuum state gives rise to $\beta_l(z,0)=\gamma_{lm}(z,0)=0$ for all m and l such that

$$|\psi(z,0)\rangle=\alpha(z,0)\ |0\rangle=\exp\{-0.5[(z-z_0)/\Delta z_i]^2+ik_iz\}\ |0\rangle \tag{4.1}$$

is just the initial Gaussian centered at $z=z_0$ with spread Δz_i and initial wave number k_i (corresponding to initial electron energy $E_i=\hbar^2k_i^2/2m$). The initial condition for the electron distribution in Eq. (3.3) is $f(k,0)=|\alpha(k,0)|^2$. In the following numerical studies, the energy and wave number results have been scaled, respectively, by $E_0\equiv\hbar\omega=36.2$ meV and $a_0\equiv\hbar/\sqrt{2mE_0}=3.975$ nm.

A. Zero electric field: Study of spontaneous LO-phonon emission

In Fig. 1 the average electron wave number $\langle k\rangle$ is shown as a function of time for initial electron energies $E_i=0.05$, 0.075, 0.10, and 0.15 eV, where (a) gives the QK results and (b) gives the SC results. The corresponding QK and SC average electron kinetic energy $\epsilon_{\rm el}$ curves are shown in Fig. 2. The initial Gaussian spread was chosen to be $\Delta k_ia_0=0.2$. The non-Markovian behavior of the kinetics can be easily seen in both QK sets of figures from the following features. In Fig. 1(a), the dissipative behavior of the electron wave number clearly deviates from the (nearly) exponential decay seen in the semiclassical results in (b). In fact, for the first few femtoseconds there is virtually no dissipation, the electron ''appears'' to propagate freely along the wire undisturbed by the lattice. Only until $t\sim 1/\omega$ (inverse phonon frequency), does the electron begin to ''feel'' the lattice and dissipate through phonon emission. Another feature is illustrated in Fig. 2(a) where in the first few femtoseconds, the electron exhibits a slight increase in energy before dissipa-

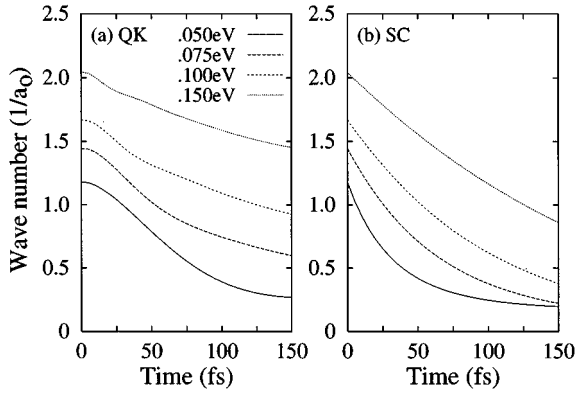

FIG. 1. Zero field case: (a) The QK and (b) the SC average electron wave number $\langle k \rangle$, as a function of time for initial electron energies $E_i = 0.05$, 0.075, 0.10, and 0.15 eV.

tion begins. This seemingly unphysical behavior is directly attributed to the time-energy uncertainty, $\Delta t \Delta \epsilon \sim \hbar$.[17,23] Classically, the final electron state, ϵ_{k-q}, is determined by selection rules governed by the energy conserving relation, $|\epsilon_k - \epsilon_{k-q} \pm \hbar\omega| = 0$. However, for small finite times, an energy uncertainty $\Delta\epsilon$ exists, allowing virtual transitions to the final state for times $\Delta t = \hbar/\Delta\epsilon$ governed by the relation $|\epsilon_k - \epsilon_{k-q} \pm \hbar\omega| = \Delta\epsilon$. These virtual transitions produce an essentially symmetrically broadened final electron state. This energy spread becomes so large at early times that the electron has an almost equal probability of gaining energy versus losing energy, causing $\epsilon_{\rm el}$ to increase but leaving $\langle k \rangle$ unchanged. Only until $t \sim 1/\omega$ does $\Delta\epsilon$ become small enough to favor transitions with an energy loss. The initial overshoot in the electron's kinetic energy can also be thought of as a decrease in it's potential energy or as a buildup of correlation. Just after $t = 0$, the electron-phonon interaction is switched on, leading to a deformation of the lattice. In other words, the electron and the phonon form a quasiparticle, the polaron. This deformation can be described by a coherent superposition of all the ''resonant'' and ''nonresonant'' (virtual) transitions to the final electron state.

The quantum-mechanical features of the electron-LO-phonon interaction discussed above are perhaps better understood from the dynamics of the correlation energy. The evolution of $\epsilon_{\rm el}$ and $\epsilon_{\rm ph}$ is shown in Fig. 3(a) for the case of $E_i = 0.10$ eV. The corresponding correlation energy ϵ_c, defined by Eq. (2.15) and by the energy conserving relation of Eq. (2.13), is plotted on a higher-energy resolution scale in Fig. 3(b). It is instructive to compare the simulated correlation energy, ϵ_c, with the early time perturbative expansion of the correlation energy of Eq. (2.15) (see Appendix B for derivation),

$$\epsilon_c^p = -2\sum_l \left(\frac{S}{Q_l}\right)^2 |A_0|^2 \left[\frac{1-\cos[(\epsilon_{k_i-q_l} - \epsilon_{k_i} + \hbar\omega)t/\hbar]}{\epsilon_{k_i-q_l} - \epsilon_{k_i} + \hbar\omega}\right], \tag{4.2}$$

which is plotted in the inset of Fig. 3(b). At $t = 0$ the system is completely uncoupled ($\epsilon_c = 0$). As time evolves, both ϵ_c and ϵ_c^p exhibit characteristic oscillations which decay to an asymptotic value. Examining Eq. (4.2) for small t, the contributions from each phonon mode, q_l, add coherently to the correlation giving rise to the negative behavior in Fig. 3(b). At later times, the contributions from the virtual transitions become randomized due to the nonzero cosine argument in Eq. (4.2). This leads to (i) effective oscillations given by the frequency, $(\epsilon_{k_i}/\hbar - \omega)$ and (ii) a diminishing amplitude in the oscillations. Therefore, the larger the initial electron energy $E_i = \epsilon_{k_i}$, the quicker the randomization and hence the faster the buildup of correlation. This behavior is reflected in Figs. 1(a) and 2(a) where the retardation of the relaxation decreases for larger E_i. In Ref. 14, Lipavský *et al.* investigated the validity of the quasiparticle approximation in equilibrium using a Green's function formalism. Their investigation led them to an analytic estimate of a quasiparticle formation time, $\tau_{\rm qp} = 2\pi\hbar/(\epsilon_k - \hbar\omega)$, which agrees well with the correlation buildup time presented here.

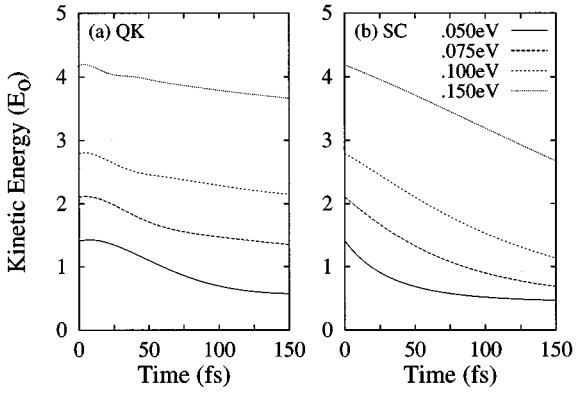

FIG. 2. Zero field case: (a) The QK and (b) the SC average electron kinetic energy $\epsilon_{\rm el}$, as a function of time for initial electron energies $E_i = 0.05$, 0.075, 0.10, and 0.15 eV.

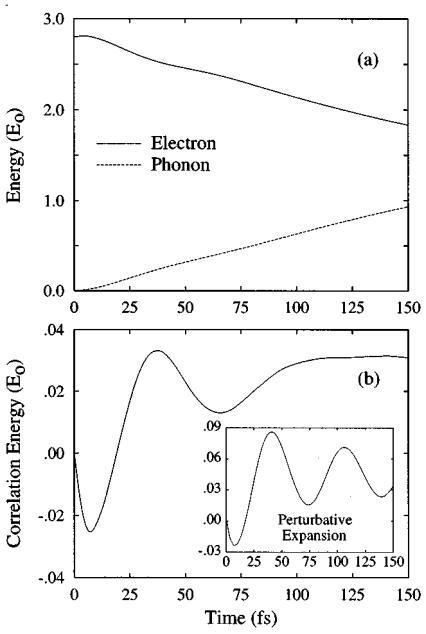

FIG. 3. (a) Comparison of the electron kinetic energy $\epsilon_{\rm el}$, with the free phonon energy $\epsilon_{\rm ph}$, as a function of time for $E_i = 0.10$ eV and (b) the corresponding electron-phonon correlation energy ϵ_c. The inset illustrates the perturbative expansion result, ϵ_c^p, derived in Appendix B.

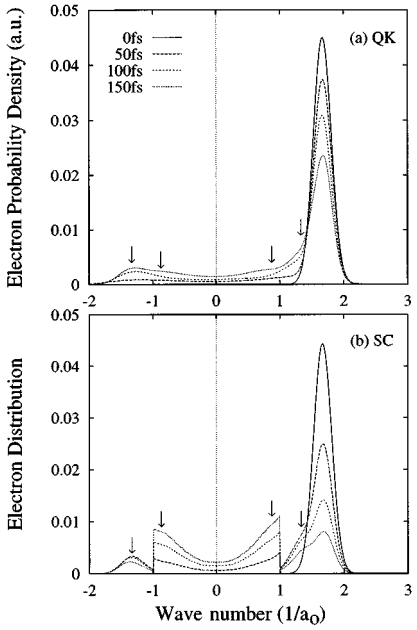

FIG. 4. Zero field case: (a) The QK electron probability distribution, $\rho_e(k,t)$, and (b) the SC electron distribution function, $f(k,t)$, as a function of wave number k for $E_i=0.10$ eV at times $t=0$, 50, 100, and 150 fs. The arrows mark the center positions of the first and second forward scattering and backscattering phonon replicas.

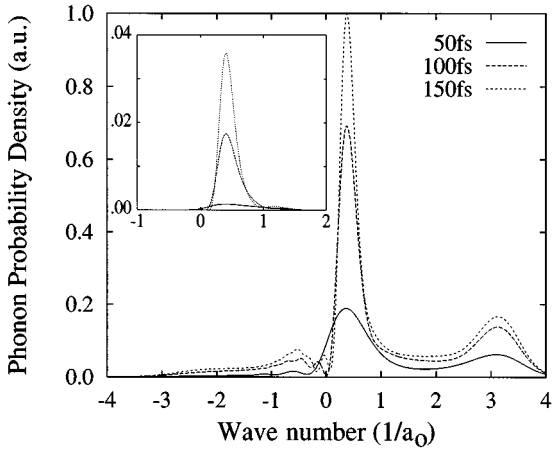

FIG. 5. Zero field case: The QK phonon probability distribution $\rho_{\mathrm{ph}_1}(k,t)$, with an occupancy of **1** in the qth mode for the case $E_i=0.10$ eV. The inset shows the contribution, $\rho_{\mathrm{ph}_2}(k,t)$, for an occupancy of **2** in the qth mode.

In the early time regime, $t<20$ fs $\sim 1/\omega$, both ϵ_c and ϵ_c^p agree comparatively well. For larger times, however, differences occur in both the frequency and amplitude of the oscillations as well as in the magnitude of the asymptotic limit. These differences stem from the limitations imposed on the correlation energy when undertaking a perturbative expansion. We note that in the derivation of Eq. (4.2), the initial electron state, $|\alpha(k,0)|^2$, was taken as a δ function and that the degrees of freedom in the system were limited to first-order number states. Accounting for an initial Gaussian state which further spreads out in time would lead to a faster randomizing of the transitions and a faster decay of the oscillations, as is evident in ϵ_c as shown in Fig. 3(b). As time evolves further, the inclusion of higher order number states is necessary for the correlation energy to approach it's true asymptotic long time limit. Observation of ϵ_c indicates that the oscillations begin to die out at a time $t\sim$ 100 fs. This suggests that for $E_i = 0.10$ eV the buildup in the electron-LO-phonon correlation takes roughly 100 fs ($\sim\tau_{\mathrm{qp}}$).

We point out that in the long time limit the sign of ϵ_c^p in Eq. (4.2) is given by the sign of $(E_i-\hbar\omega)$. This means that ϵ_c^p is negative when the initial electron energy E_i is below the phonon threshold and ϵ_c^p is positive when E_i is above it.[28]

Comparing the QK and SC electron energy curves in Fig. 2 we note that the energy relaxation is much less pronounced in the QK case. For example, an electron initially with $E_i=2.77\hbar\omega$ loses only $0.57\hbar\omega$ after 150 fs in the QK case whereas it loses $1.57\hbar\omega$ in the SC case. This large difference can be explained by comparing the corresponding QK and SC electron probability distributions, shown in Fig. 4. In (a), the QK curve for $t=50$ fs illustrates a large, nearly structureless spread, in the distribution of final electron states (due to the time-energy uncertainty as discussed previously). Only until later times ($t\sim$ 100 fs) does a reshaping occur at the first phonon replica at $ka_0=\pm 1.33$. And further, transitions into the second phonon replica at ($ka_0=\pm 0.83$) do not appear until times $t\sim$ 150 fs. Even after 150 fs the distribution of final electron states remains wide and structureless across the LO-phonon emission spectrum. In sharp contrast the SC curves in Fig. 4(b) illustrate an almost immediate appearance of the well-defined first and second phonon replicas. In addition, the transitions into the first replica are short lived and are quickly transferred to the second replica. Furthermore, in the QK simulation, even after 150 fs the electron still has a significant probability of remaining in it's initial state, while in the SC simulation this probability is much smaller. The sharp discontinuities in Fig. 4(b) reflect the LO-phonon threshold at $ka_0=1$, whereas the wave nature of the electron which is naturally accounted for in the QK model completely smooths out this singularity. This nicely demonstrates that in the QK treatment the electron is never in a well-defined state. The initial wave packet broadens further due to collisions. However, the electron remains in a continuously changing, but still coherent, superposition of states.

A similar statement holds for the phonon system where the electron always interacts with many phonon states and the phonon system itself is also in a coherent superposition of many states. The evolution of the phonon probability distribution also illustrates this slow transition to the first and second phonon replicas. The probability for finding phonon occupancies of **1** and **2** in the kth mode, denoted, respectively, by $\rho_{\mathrm{ph}_1}(k,t)$ and $\rho_{\mathrm{ph}_2}(k,t)$, are shown in Fig. 5. The phonon distribution exhibits the similar narrowing (in time) into peaked structures about the k states associated with the phonon replicas seen in Fig. 4(a). Furthermore, the contribution of having two phonons in the same state is very small on these short time scales, as seen in the inset in Fig. 5.

B. External dc electric field: Intracollisional field effect

We now consider an external dc electric field, F, applied along the wire length. In Fig. 6 the QK (a) and SC (b) time

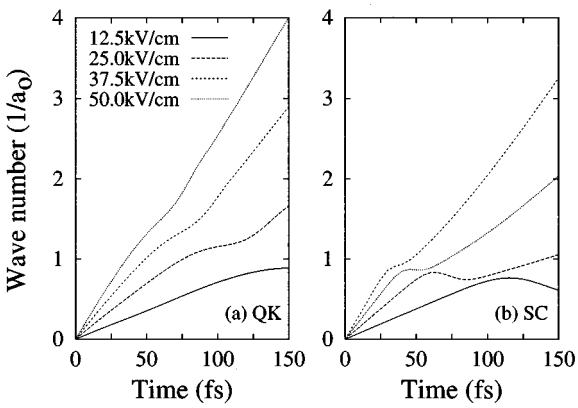

FIG. 6. External field case: (a) The QK and (b) the SC average electron wave number $\langle k \rangle$, as a function of time for $E_i = 0$ and electric field strengths $F = 12.5$, 25, 37.5, and 50 kV/cm.

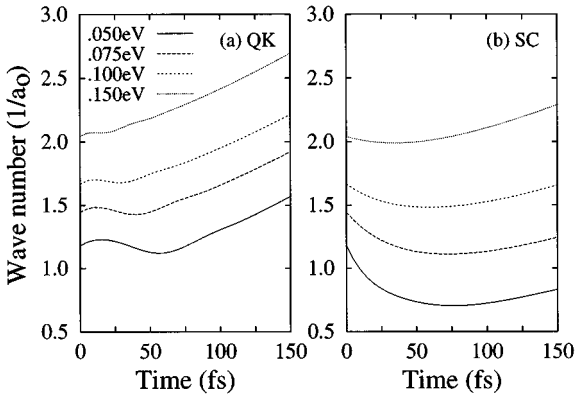

FIG. 7. External field case: (a) The QK and (b) the SC average electron wave number $\langle k \rangle$, as a function of time for initial electron energies $E_i = 0.05$, 0.075, 0.10, and 0.15 eV and an electric field strength of $F = 12.5$ kV/cm.

evolution of $\langle k \rangle$ is shown for different field strengths for an electron initially at rest. In both (a) and (b), early on the electron linearly accelerates with the field. However, striking differences between the QK and SC simulations occur as the electron approaches the phonon threshold. For the SC case, a distinct ''kink'' occurs *below* the phonon threshold, where the larger the field, the shorter the lifetime of the kink. The onset of the kink occurs when the high-energy edge of the electron distribution $f(k,t)$ is accelerated past the phonon threshold and the kink vanishes when the low-energy edge of $f(k,t)$ has passed the threshold. On the other hand, for the QK case the effect of the interaction produces a much more broadened kink that extends both later in time and for wave numbers *above* the phonon threshold. This is a direct consequence of the continuous and simultaneous nature of the electron's acceleration in the electric field and the electron-phonon interaction. A comparison of (a) and (b) clearly indicates the presence of the intracollisional field effect (ICFE), especially for the strongest field case, $F = 50$ kV/cm. The independent treatment of electron acceleration and electron scattering in semiclassical kinetics causes a much stronger scattering effect (suppression of transport), while the QK curve resembles nearly ballistic behavior. In this case the interaction is unable to build up in the short time scale set by the large electric field, causing the electron to quickly runaway with the field.

The importance of the ICFE is also seen for the model transport problem where the carrier is injected in the wire with a finite energy. Figure 7 shows the QK (a) and SC (b) $\langle k \rangle$ curves for different initial energies, E_i, in the presence of a 12.5 kV/cm electric field. Again, in the QK simulation a direct transition from the interaction buildup phase to the runaway phase can be observed which favors ballistic transport.

V. CONCLUSION

We presented a quantum kinetic theory, based on the many-body Schrödinger equation, for the early time kinetics of an electron in a quantum wire that is coupled to the spectrum of LO-phonon modes. We demonstrated that the computation of the many-body wave function is feasible for early times. This direct approach has the advantage of including all correlations between the electron and the phonons. It was shown that some of the special features of early time kinetics are directly caused by the buildup of these correlations. These features were (i) a delayed loss of the average electron momentum and (ii) initial overshoots of the average electron kinetic energy. We showed that these effects are mediated mainly by the emission and absorption of *virtual* phonons. On the other hand, the semiclassical Boltzmann equation neglects virtual transitions and treats phonon emission and absorption as independent processes. This is in clear contrast to quantum kinetics, where real and virtual transitions cannot be treated separately since scattering and energy renormalization are different aspects of the same interaction process. Emission and absorption of phonons are also interdependent processes because in a virtual process a phonon emission has to be ''undone'' by it's inverse absorption and visa versa.

In our study we assumed an initially uncoupled electron-phonon system. Thus we where able to monitor the correlation buildup, which is nothing but the transformation of a free particle into a quasiparticle, the polaron. The quantum kinetic treatment shows that on a microscopic level the interaction process is continuous. Once the correlations are built up the electron and the phonons stay correlated. This again is in contrast to the semiclassical picture of the interaction process which is assumed to be a chain of individual events: A free electron enters an ''interaction zone'' and becomes correlated with the lattice, which eventually leads to the emission or absorption of a phonon. Then all correlations vanish and the electron leaves the zone as a free particle and the process starts all over again. In the derivation of the Boltzmann scattering integrals it is crucial to assume that the time the electron spends in the interaction zone (the collision duration time) is much smaller than the time between successive scattering events (the inverse scattering rate). This crucial difference between quantum kinetics and the semiclassical kinetic picture explains why it is so difficult, if not impossible, to find a direct quantum kinetic definition of the collision duration time. Lipavský *el al.*[14] suggested that the quasiparticle formation time should be regarded as the quantum kinetic analogy of the semiclassical collision duration time. Using this definition, we find that the collision duration time and the inverse scattering rate are actually of similar

magnitude, showing again the importance of virtual transitions leading to (in the language of semiclassical kinetic theory) energy-renormalization and multiple phonon scattering effects.

It was further shown that the continuous nature of the interaction also has strong implications on the behavior of the electron in a longitudinal electric field. If the field is strong enough to accelerate the electron considerably, on a time scale set by the quasiparticle formation time, phonon scattering becomes ineffective. Semiclassical theory neglects this intracollisional field effect and thus overestimates the effects of phonon scattering in the presence of a strong field.

ACKNOWLEDGMENTS

The author would like to thank Dr. K. El Sayed, Dr. A. V. Kuznetsov, Professor C. J. Stanton, and Professor T. K. Gustafson for many helpful and enlightening discussions. This work was supported by the Department of Energy, Office of Basic Energy Sciences, Grant No. DE-FG05-91-ER45462.

APPENDIX A: PHONON MODE PROBABILITY DISTRIBUTION

We illustrate the calculation of the phonon distribution with a simple example. Consider the many-body wave function for a system with a total number of $N=3$ phonon modes according to Eq. (2.7), truncated to second-order lattice number states,

$$\begin{aligned}|\psi(z,t)\rangle = {} & \alpha(z,t)|000\rangle+\beta_1(z,t)|100\rangle+\beta_2(z,t)|010\rangle \\ & +\beta_3(z,t)|001\rangle+\gamma_1(z,t)|110\rangle+\gamma_2(z,t)|101\rangle \\ & +\gamma_3(z,t)|011\rangle+\gamma_4(z,t)|200\rangle+\gamma_5(z,t)|020\rangle \\ & +\gamma_6(z,t)|002\rangle.\end{aligned}$$

In general, $\rho_{\mathrm{ph}_i}(q_j,t)$ is defined as the probability of finding phonon mode q_j with an occupancy i at time t. Thus as an example, the probability of finding phonon mode q_1 with an occupancy of **0** as a function of time is given as

$$\begin{aligned}\rho_{\mathrm{ph}_0}(q_1,t) = \int dz[& |\alpha(z,t)|^2+|\beta_2(z,t)|^2+|\beta_3(z,t)|^2 \\ & +|\gamma_3(z,t)|^2+|\gamma_5(z,t)|^2+|\gamma_6(z,t)|^2]. \quad \text{(A1)}\end{aligned}$$

The time evolution of the phonon probability distribution is formed by taking the spectrum of probabilities ρ_{ph_i}, for a particular mode occupancy, and plotting them versus the wave number k.

APPENDIX B: PERTURBATIVE EXPANSION OF THE CORRELATION ENERGY

The analytical calculation for the correlation energy of the electron-LO-phonon interaction, ϵ_c, is presented for the case of early time kinetics. The correlation energy is defined as

$$\epsilon_c = \langle \psi(z,t)|\hat{H}_{e-\mathrm{ph}}|\psi(z,t)\rangle, \quad \text{(B1)}$$

where $|\psi(z,t)\rangle$ and $\hat{H}_{e-\mathrm{ph}}$ are given, respectively, by Eqs. (2.4) and (2.7). Performing the necessary Boson operations defined in Sec. II, we obtain

$$\begin{aligned}\epsilon_c(t) = S\int dz\Bigg\{ & ie^{-i\omega t}\sum_l \frac{e^{iq_l z}}{Q_l}\Bigg[\alpha^*(z,t)\beta_l(z,t) \\ & +\sqrt{2}\beta_l^*(z,t)\gamma_{ll}(z,t)+\sum_{m>l}\beta_m^*(z,t)\gamma_{lm}(z,t) \\ & +\sum_{m<l}\beta_m^*(z,t)\gamma_{ml}(z,t)\Bigg]+\text{c.c.}\Bigg\}, \quad \text{(B2)}\end{aligned}$$

where c.c. denotes the complex conjugate. Our goal is to obtain an analytic expression for ϵ_c for the early times. Therefore we ignore all contributions from second-order transitions in Eq. (B2) by neglecting all terms with the coefficient γ. Taking the Fourier transform of this truncation yields,

$$\begin{aligned}\epsilon_c(t) = S\Bigg[& ie^{-i\omega t}\sum_l \frac{1}{Q_l}\sum_k \alpha^*(k+q_l,t)\beta_l(k,t) \\ & -ie^{i\omega t}\sum_l \frac{1}{Q_l}\sum_k \beta_l^*(k+q_l,t)\alpha(k,t)\Bigg]. \quad \text{(B3)}\end{aligned}$$

In order to obtain our goal, we solve Eq. (B3) perturbatively. The zeroth-order solution to $\alpha(k,t)$ is $A_k\exp[-i\epsilon_k t/\hbar]$, with $A_k=\alpha(k,0)=\exp[(k-k_i)^2/2(\Delta k)^2]$, see Eq. (4.1). The first-order solution to $\beta_l(k,t)$ is obtained by integrating

$$\frac{\partial\beta_l(k,t)}{\partial t} = \frac{\epsilon_k}{i\hbar}\beta_l(k,t)-\frac{Se^{i\omega t}}{\hbar Q_l}\alpha(k+q_l,t),$$

which is just the Fourier transform of Eq. (2.9), where only up through the first-order interaction terms have been retained and where $V_z=0$. Simple integration leads to

$$\beta_l(k,t) = -\frac{SA_{k+q_l}}{iQ_l}\frac{e^{-i(\epsilon_{k+q_l}-\hbar\omega)t/\hbar}-e^{-i\epsilon_k t/\hbar}}{\epsilon_k-\epsilon_{k+q_l}+\hbar\omega}. \quad \text{(B4)}$$

Before proceeding we simplify the calculation by further assuming that the initial electron state is represented by a δ function,

$$|A_{k+q_l}|^2 \sim |A_0|^2 L\ \delta_{k+q_l,k_i}.$$

Inserting Eq. (B4) into Eq. (B3) and using the above assumption yields the analytic expression for the correlation energy for the early times, given in Eq. (4.2).

[1] K. Seeger, *Semiconductor Physics*, 3rd ed. (Springer, Berlin, 1985).
[2] J. Collet, T. Amand, and M. Pugnet, Phys. Lett. **96A**, 368 (1983).
[3] J. Collet, J.L. Oudar, and T. Amand, Phys. Rev. B **34**, 5443 (1986).
[4] C.J. Stanton, D.W. Bailey, and K. Hess, IEEE J. Quantum Electron. **24**, 1614 (1988).
[5] L. Rota, P. Lugli, T. Elsässer, and J. Shah, Phys. Rev. B **47**, 4226 (1993).
[6] K.W. Kim, M.A. Stroscio, A. Bhatt, R. Mickevicius, and V.V. Mitin, J. Appl. Phys. **70**, 319 (1991).
[7] G. Böhne, T. Sure, R.G. Ulbrich, and W. Schäfer, Phys. Rev. B **41**, 7549 (1990).
[8] R.L. Fork, C. Cruz, P.C. Becker, and C.V. Shank, Opt. Lett. **12**, 483 (1987).
[9] P.C. Becker, H.L. Fragnito, R.L. Fork, F.A. Beisser, and C.V. Shank, Appl. Phys. Lett. **54**, 411 (1989).
[10] L. Bányai, D.B. Tran Thoai, E. Reitsammer, H. Haug, D. Steinbacher, M.U. Wehner, M. Wegener, T. Marschner, and W. Stoltz, Phys. Rev. Lett. **75**, 2188 (1995).
[11] L. Reggiani, P. Lugli, and A.P. Jauho, Phys. Rev. B **36**, 6602 (1987).
[12] D.W. Bailey, C.J. Stanton, and K. Hess, Phys. Rev. B **42**, 3423 (1990).
[13] P. Lipavský, F.S. Khan, F. Abdolsalami, and J.W. Wilkins, Phys. Rev. B **43**, 4885 (1991).
[14] P. Lipavský, F.S. Khan, and J.W. Wilkins, Phys. Rev. B **43**, 6650 (1991).
[15] R. Zimmermann, Phys. Status Solidi B **159**, 317 (1990).
[16] R. Zimmermann, J. Lumin. **53**, 187 (1992).
[17] J. Schilp, T. Kuhn, and G. Mahler, Phys. Rev. B **50**, 5435 (1994).
[18] A.V. Kuznetsov, Phys. Rev. B **44**, 8721 (1991).
[19] H. Haug, Phys. Status Solidi B **173**, 139 (1992).
[20] A.V. Kuznetsov, Phys. Rev. B **44**, 13 381 (1991).
[21] K. El Sayed, L. Bányai, and H. Haug, Phys. Rev. B **50**, 1541 (1994).
[22] H. Haug and C. Ell, Phys. Rev. B **46**, 2126 (1992).
[23] J.A. Kenrow and T.K. Gustafson, Phys. Rev. Lett. **77**, 3605 (1996).
[24] This corresponds to replacing $\hat{H}_{e-\mathrm{ph}}(x,y,z)$ in Ref. 25 by it's transversal average $\hat{H}_{e-\mathrm{ph}}(z)$, see Eq. (2.4).
[25] M.A. Stroscio, Phys. Rev. B **40**, 6428 (1989).
[26] S. Briggs, B.A. Mason, and J.P. Leburton, Phys. Rev. B **40**, 12 001 (1989).
[27] T. Meier, G. von Plessen, P. Thomas, and S.W. Koch, Phys. Rev. Lett. **73**, 902 (1994).
[28] This behavior may be compared to a boat moving in water. A slow moving boat displaces the water and loses potential energy while a fast moving boat is lifted by its own bow wave.